Scanning probe method investigation of carbon nanotubes produced by high energy ion irradiation of graphite

L.P. Biró[a,d,*], G.I. Márk[a], J. Gyulai[a,c], N. Rozlosnik[b], J. Kürti[b], B. Szabó[a,b], L. Frey[c], H. Ryssel[c]

[a]*Research Institute for Technical Physics and Materials Science, H-1525 Budapest, P.O. Box 49, Hungary*
[b]*Eötvös University, Department of Biological Physics, H-1088 Puskin u.5-7, Hungary*
[c]*FhG-Institut für Integrierte Schaltungen, 91058 Erlangen, Schottkystr 10, Germany*
[d]*Facultes Universitaires Notre Dame de la Paix, LASMOS, 5000 Namur, Rue de Bruxelles 61, Belgium*

Abstract

Carbon nanotubes were evidenced by atomic force microscopy and scanning tunneling microscopy on highly oriented pyrolytic graphite irradiated with high energy ions (215 MeV Ne, 209 MeV Kr, 246 MeV Kr, and 156 MeV Xe). On the samples irradiated with Kr and Xe ions, craters attributed to sputtering were found. Frequently, one or several nanotubes emerge from these sputtering craters. Some of the observed nanotubes vibrate when scanned with the AFM. Except nanotubes, no other deposits were observed. © 1999 Elsevier Science Ltd. All rights reserved.

1. Introduction

Since their discovery in 1991 by Iijima [1], due to their remarkable properties [2,3], a continuously growing interest is focused onto the carbon nanotubes (CNT). Recent experimental results proved an excellent agreement between theoretical predictions [4] and the electronic structure of single-walled carbon nanotubes (SWNT) probed by scanning tunneling spectroscopy (STS) [5,6]; experimental evidence pointing to the feasibility of CNT based nanoelectronics were reported [7,8].

The most frequently used procedures to produce large amounts of carbon nanotubes are: the electric arc method [9], laser ablation [10], and the catalytic decomposition of hydrocarbons [11]. All these methods yield amorphous carbon and graphitic material together with the CNT. Tedious purification steps are needed to obtain a material which contains only CNTs. In the electric arc, and in the laser ablation methods, the growth of carbon nanotubes takes place in a highly excited carbon plasma generated at several thousands °C, while the catalytic process is based on the dehydrogenation at 700°C of hydrocarbons. In the present paper we report a new procedure for the production of carbon nanotubes which is based on the irradiation of highly oriented pyrolytic graphite (HOPG) targets with high energy ($E > 100$ MeV) heavy ions. Individual CNTs of several μm in length are observed by atomic force microscopy (AFM) and scanning tunneling microscopy (STM) in, or around the craters where higher order, dense nuclear cascades – the so called Brinkman type cascades [12] – intersected the sample surface and produced extended sputtering. Frequently, the CNTs traversing surface features on the HOPG vibrate when scanned with a tapping mode (TM) AFM.

2. Experimental results and discussion

The HOPG samples were irradiated with low dose, typically 10^{12} cm^{-2}, of 215 MeV Ne, 209 MeV and 246 MeV Kr and 10^{11} cm^{-2} 165 MeV Xe ions. The samples were freshly cleaved before irradiation and were handled with maximum care after irradiation to avoid any surface contamination. It is worth mentioning that in the last years

---

*Corresponding author. Tel: +36-1-3959220; fax: +36-1-3959284.
E-mail address: biro@mfa.kfki.hu (L.P. Biro)

we investigated in some detail the interaction of swift, heavy ions with crystalline targets, like: Si [13,14], muscovite mica [15], and HOPG [16,17]. Usually, Si, mica and HOPG samples were irradiated simultaneously, during the same run. While no CNTs were found on any of the Si or mica samples, on every HOPG sample we found CNTs.

The irradiated samples were investigated in ambient atmosphere using contact mode (CM) and tapping mode (TM) atomic force microscopy, and scanning tunneling microscopy. For AFM measurements blunt tips ($R > 100$ nm) were preferred because the convolution effect of the tip shape with the tube shape produces the apparent widening of the tube in the horizontal plane. This facilitates finding the CNTs in large scan windows of the size of 100 μm^2. The STM tips were mechanically prepared Pt tips, the tunneling parameters used were similar to those commonly used for HOPG: tunneling current of 1 nA, and bias of 100 mV.

In Fig. 1 a TM-AFM image of a sputtering crater on the surface of HOPG irradiated with Xe ions is shown, the total length of the carbon nanotube emerging from the crater is 11 μm, the diameter of the CNT as measured from its height – the height is not influenced by convolution effects – is 6 nm in the vicinity of the crater and gradually decreases to 1 nm in the end region. As shown by the line cut in Fig. 1, the tube height as measured along the tube axis shows a regular oscillation pattern. It is worth pointing out that the edge of the crater does not show any oscillatory behavior, i.e., the oscillation of the CNT is not an imaging artifact. Assuming a conic shape for the crater, its estimated volume is 1.4×10^{-3} μm^3, this means that 1.6×10^8 carbon atoms were sputtered away. Taking the CNT in Fig. 1 as being a double wall tube, and assuming that all the atoms will be built into CNTs, 20 similar CNTs could be generated from the C atoms sputtered out of the crater, if the density of bulk graphite is used, this number decreases to 14.

Those sputtered atoms which have a significantly higher energy will quickly leave the vicinity of the surface, while the less energetic ones, and the clusters, will form an expanding cloud in which the nanotube growth may take place. After the fast growth in the expanding cloud takes place, the nanotube will collapse onto the surface, where additional growth may take place due to the target atoms ejected at very low energies in those collisions which are responsible for the generation of the well known hillocks on ion bombarded HOPG [18]. For example, in the case of 246 MeV Kr irradiation it is found by STM examination that 10^2 μm^{-2} hillocks are produced, while the density of carbon nanotubes found is 2×10^{-3} μm^{-2}. For a dose ten times lower, in the case of Xe irradiation a slightly higher nanotube density in the range of 3×10^{-3} μm^{-2} was found.

It was frequently observed that especially those carbon nanotubes, which cross elevated surface features, like cleavage steps or folds on HOPG, oscillate when scanned

with the AFM. A TM-AFM image showing this phenomenon is presented in Fig. 2, the image was not filtered in any way. One can note that the step crossing the image does not show any vibration, the nanotube crosses the step close to the left hand edge of the image. The total length of the nanotube exceeds 100 μm, its diameter is estimated to be 36 nm, the vibration causes some incertitude in the accuracy of this value.

To get a better insight into how the TM-AFM generates the image of a vibrating object, computer modeling was used. As a first approximation a simple model consisting of a cylindrical rod of 36 nm diameter performing a transversal lateral sinusoidal vibration was used. The rod is placed on a flat support surface along the y direction. The scan direction was perpendicular to the rod axis. The scan was performed in a window of 50×50 μm^2 at a scan frequency of 1 Hz by a tip of spherical shape with a radius of 300 nm. The window was sampled in 256×256 pixels, with an averaging of 64 kHz, the sampling frequency used in the TM-AFM. We have assumed that in each sampling point the tip is descending until it touches the sample. From this assumption for a cylindrical rod of radius R_{rod} at position x_{rod} and a spherical tip of radius R_{tip} at lateral position (x_{tip}, y_{tip}) the apparent tip height above the rod is obtained as:

$$z_{tip} = [(R_{rod} + R_{tip})^2 - (x_{rod} - x_{tip})^2]^{(1/2)} - R_{rod}, \qquad (1)$$

where

$$x_{rod} = A \sin(2\pi f t), \qquad (2)$$

and x_{tip} is increasing linearly in each scan line with a scan speed of $v_{tip} = 100$ $\mu m/s$.

From this simple model similar vibration patterns like those measured experimentally were obtained, a 3D presentation comparable with Fig. 2 is shown in Fig. 3. To make a semiquantitative comparison we used the spatial period of 5 μm and corrugation amplitude of 15 nm determined from an experimental line cut drawn along the tube axis. From these parameters we have obtained $f = 1/51.2$ Hz and $A = 96.5$ nm for the vibration frequency and amplitude of the rod. The surprisingly low vibration frequency may be a consequence of the 'friction' of the nanotube with the supporting surface [19,20]. Further work is needed to built models that take in account these interactions and simulate in a more realistic way the dissipation of the vibration energy fed in the cantilever-tip system.

We finally consider a possible scenario for the crater formation and material sputtering. There are two mechanisms by which an energetic particle moving in a solid may transfer enough energy to the solid to induce structural modifications: (i) the electronic stopping mechanism (inelastic interaction with the electrons of the target atoms), typical for high energy particles ($E > 1$ MeV); and (ii) the nuclear stopping mechanism (elastic collisions with
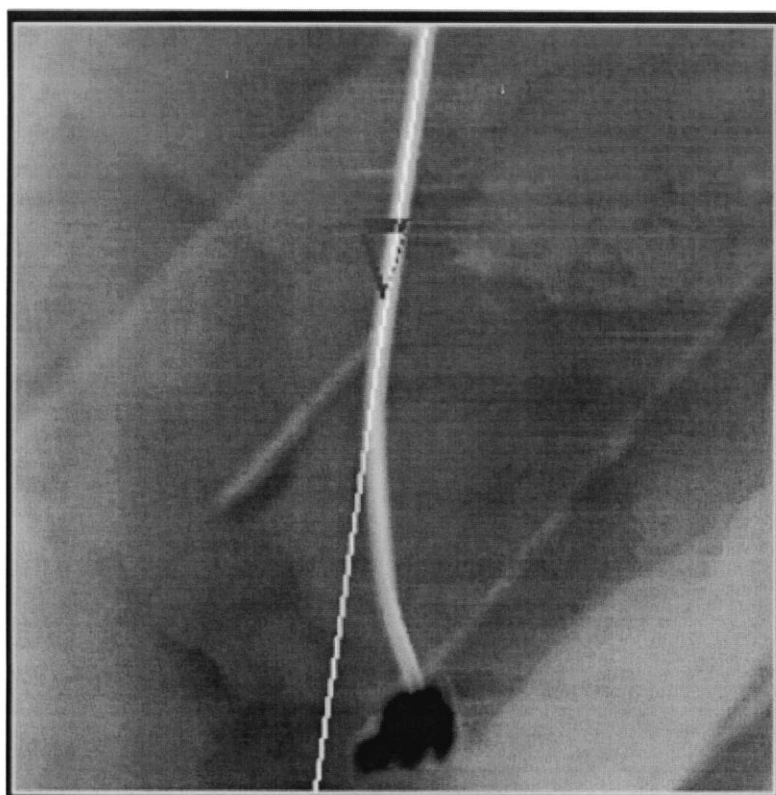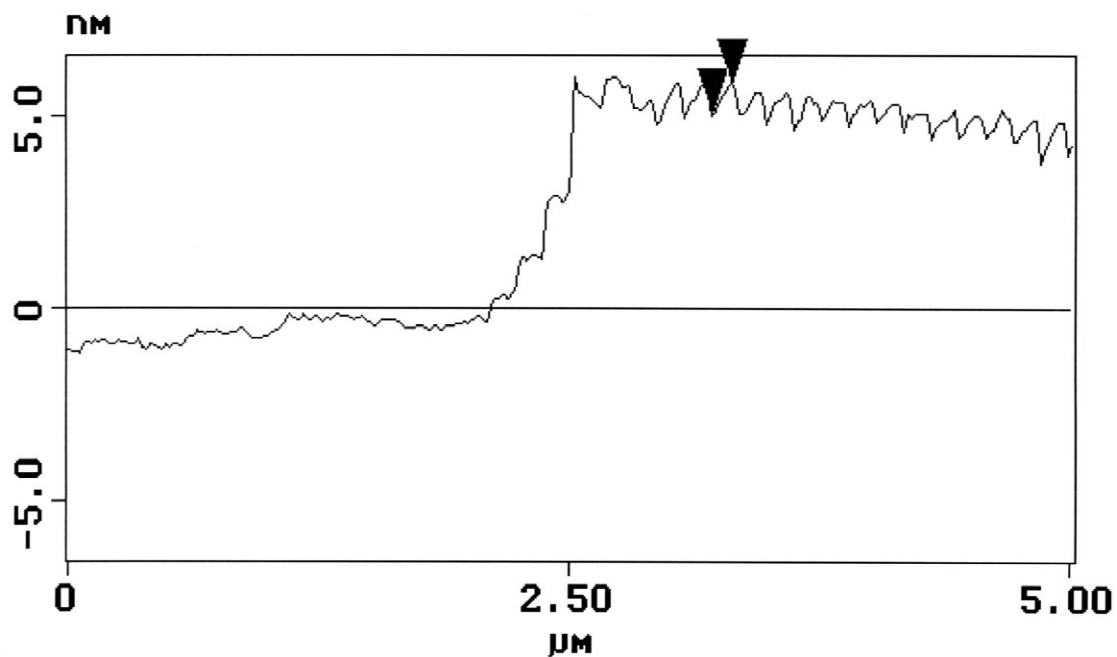
Fig. 1. Tapping mode AFM image of a sputtering crater and of a nanotube emerging from the crater on the surface of HOPG irradiated with Xe ions. The line cut over the image shows the presence of a regular oscillation pattern along the tube axis. The vertical amplitude of the oscillation is 0.7 nm, while its spatial period is 194 nm.
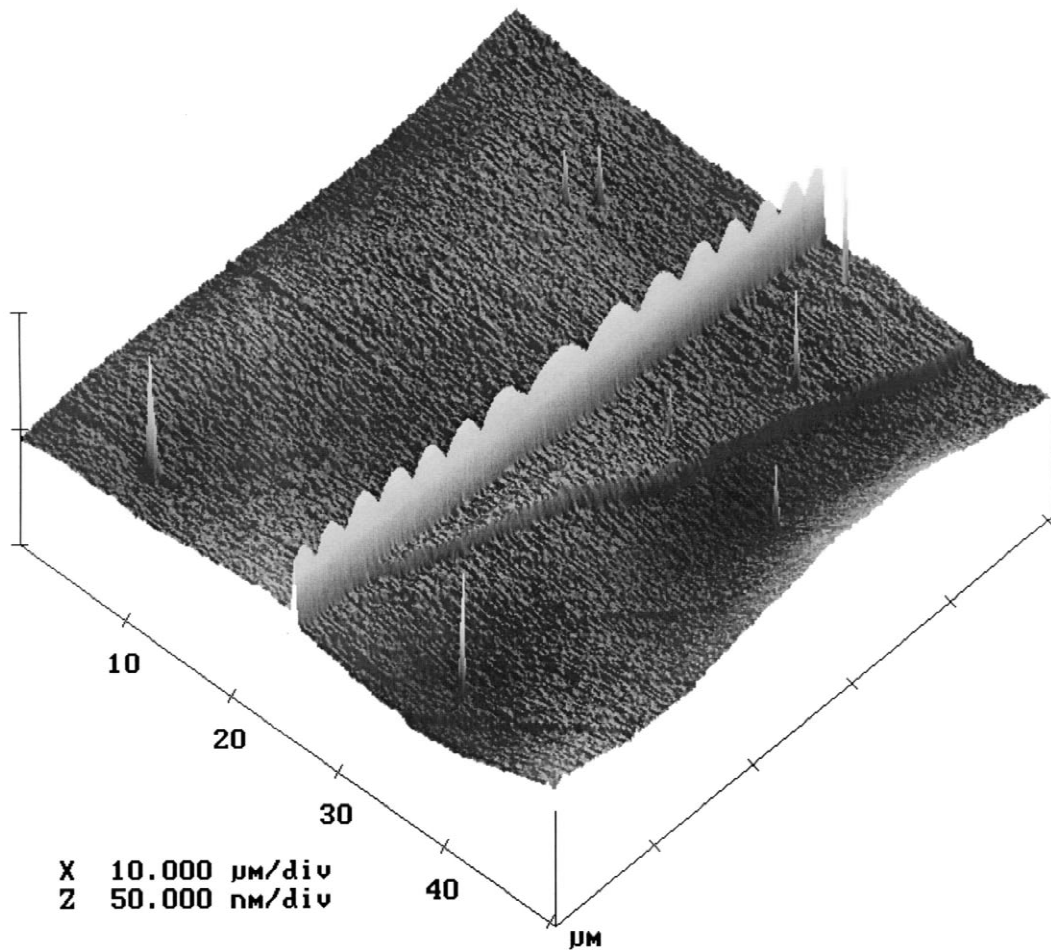
Fig. 2. 3D presentation of tapping mode AFM image acquired on HOPG irradiated with Kr ions, unfiltered image. Note the simultaneous presence of a step which is immobile in the image, and of a carbon nanotube, which shows a regular oscillation pattern. The diameter of the nanotube is estimated to be 36 nm.

the nuclei of the target atoms) dominant for low energy particles. The high energy ions used in the present work, when falling on the target surface, they all have energies in the dominant electronic stopping regime. So, if this mechanism would be responsible for the crater production, every incident ion should generate a crater. The surface densities of the craters when Kr or Xe ions were used, were in the range of 10^{-3} μm^{-2}, this means that for example in the case of Kr ions every 10^7 ions produces an event that leads to a surface crater. Therefore, the crater production and surface sputtering is attributed to those knocked-on target atoms which are produced by elastic collisions in deeper regions of the target, in higher order cascades. These target atoms are displaced by other target atoms which have gained kinetic energy in earlier colli-sional processes. Some of the C atoms knocked-on in the higher order collisions may take an outward pointing direction, intersecting the irradiated surface. If such a knocked-on atom generates in turn several sub-cascades in

a limited region, which are active in the same time, this may lead to extended surface sputtering in that region where the simultaneously active sub-cascades cross the target surface [21]. In an earlier work we reported TM-AFM images of the surface termination of dense nuclear cascades in Si and muscovite mica [22], in which numer-ous satellites are clearly visible around the main cascade. Due to the particular structure of HOPG this kind of cascades may produce the observed craters. Although, at the present moment the above detailed scenario seems to be the most realistic one that accounts for the crater production, some synergistic interaction of electronic and nuclear stopping effects may not be excluded.

In order to get additional proof that the observed objects are different from surface folds on HOPG, some of the nanotubes and an object, clearly identified as a surface fold, were cut by a focused ion beam (FIB) apparatus and the section was examined by the scanning electron micro-scope built into the FIB. When comparing cut nanotubes
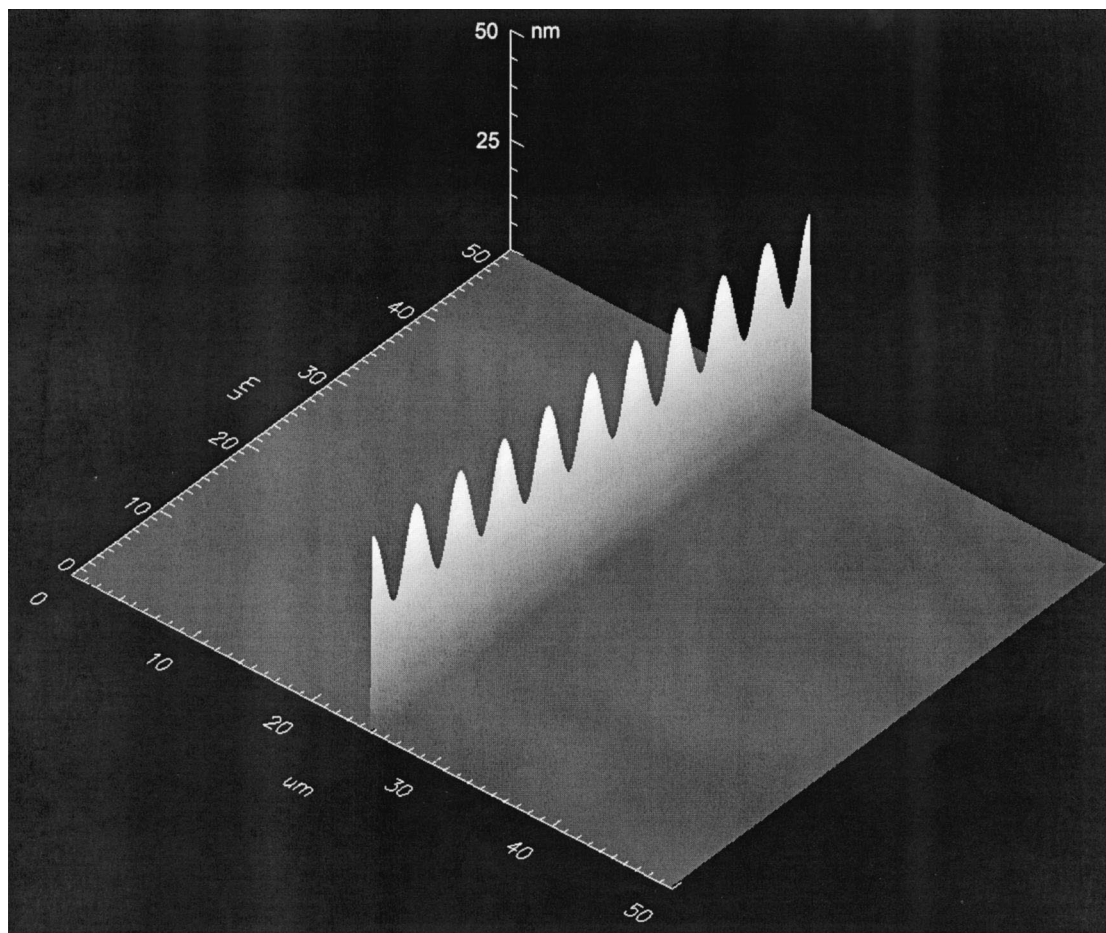
Fig. 3. Computer simulation of the image of a vibrating rod in the tapping mode AFM. An amplitude of 15 nm and a spatial period of 5 μm were chosen for the rod for easier comparison with the experimental image shown in Fig. 2.

with the fold, clear differences were found in the cross-sectional structure of these objects [21].

3. Conclusions

Carbon nanotubes of several μm in length, produced from target atoms sputtered by dense, nuclear cascades were evidenced by AFM and STM investigation of HOPG targets irradiated with high energy, heavy ions. The formation of other carbon based structures, like graphitic particles or amorphous carbon was not observed. This is an indication that using ion beam techniques carbon nanotubes may be produced in a way which makes possible the avoidance of purification steps.

Frequently, one or several nanotubes were found to emerge from the sputtering craters. Several vibrating nanotubes were observed, a comparison with a simple computer model of the image generation of a vibrating rod in a TM-AFM indicates an oscillation frequency of the order of 0.02 Hz. The extremely low frequency is tenta-

tively attributed to the interaction of the nanotube with the support.

References

[1] Iijima S. Nature 1991;354:56.
[2] Dresselhaus MS, Dresselhaus G, Eklund PC. Science of fullerenes and carbon nanotubes. San Diego: Academic Press, 1996.

[3] Ebbesen ThW, editor. Carbon nanotubes preparation and properties. Boca Raton: CRC Press, 1997.

[4] Mintmire JW, Dunlap BI, White CT. Phys Rev Lett 1992;68:631.

[5] Wildöer JWG, Venema LC, Rinzler AG, Smalley RE, Dekker C. Nature 1998;391:59.

[6] Odom TW, Huang J-L, Kim Ph, Lieber ChM. Nature 1998;391:62.

[7] Collins PhG, Zettl A, Brando H, Thess A, Smalley RE. Science 1997;278:100.

[8] Tans SJ, Verschueren ARM, Dekker C. Nature 1998;393:49.

[9] Ebbesen TW, Hiura H, Fujita J, Ochiai Y, Matsui S, Tanigaki K. Chem Phys Lett 1993;209:83.

[10] Thess A, Lee R, Nikolaev P, Dai H, Petit P, Robert J, Xu C, Lee YH, Kim SG, Rinzler AG, Colbert DT, Scuseria GE, Tománek D, Fischer JE, Smalley RE. Science 1996;273:483.

[11] Ivanov V, B Nagy J, Lambin Ph, Lucas A, Zhang XB, Zhang XF, Bernaerts D, Van Tendeloo G, Amellinckx S, Van Landuyt J. Chem Phys Lett 1994;223:329.

[12] Brinkman AJ. Am J Phys 1956;25:961.

[13] Biró LP, Gyulai J, Havancsák K, Didyk AYu, Bogen S, Frey L. Phys Rev 1996;B 54:11853.

[14] Biró LP, Gyulai J, Havancsák K, Didyk AYu, Frey L, Ryssel H. Nucl Instr Meth B 1997;127–128:32.

[15] Biró LP, Gyulai J, Havancsak K. Nucl Instr Meth 1997;B 122:476.

[16] Biró LP, Gyulai J, Havancsák K. Phys Rev 1995;B 52:2047.

[17] Ziegler JP, Biersack JP, Littmark V. The stopping and range of ions in solids I and II. New York: Pergamon Press, 1986.

[18] Coratger R, Claverie A, Ajustron F, Beauwillain J. Surf Sci 1990;227:7.

[19] Falvo MR, Clary GJ, Taylor RM, Chi V, Brooks Jr. FP, Washburn S, Superfine R. Nature 1997;389:582.

[20] Wong EW, Sheenan PE, Lieber ChM. Science 1997;277:1971.

[21] Biró LP, Márk GI, Gyulai J, Havancsák K, Lipp S, Lehrer Ch, Frey L, Ryssel H. Nucl. Instr. Meth. B: in press.

[22] Biró LP, Gyulai J, Havancsák K. Vacuum 1998;50:263.